Multi-view Privileged Information-based Representation Learning for Liver Cancer Diagnosis

Bangming Gong✉ GBM351SHU@GMAIL.COM
College of Science & Technology Ningbo University, Ningbo, 315300, China
Shanghai University, Shanghai, 200444, China

Yan Huo HUOYENN@QQ.COM
Nanjing University, Nanjing, 210093, China

Editors: Hung-yi Lee and Tongliang Liu

Abstract

Privileged information (PI) provides additional knowledge to improve performance. Though some efforts are carried out by learning using privileged information (LUPI), they mainly focus on classifier-level LUPI and single-view PI tasks. Therefore, it is a challenge for feature representation learning by transferring multi-view PI to improve the main view. In this paper, we propose a novel feature-level LUPI for multi-view PI tasks, called the multi-view privileged information-based representation learning (MPIRL) algorithm, in which multi-view PI and main view are required at the training phase, but only the main view is available at the testing phase. MPIRL consists of a feature-level LUPI module and a classification module. The feature-level LUPI module of MPIRL designs a multi-branch structure to transfer the multi-view privileged information to the main view, so that diversity and discriminative representation can be generated. For the classification module, multi-view deep SVM (MDSVM) is developed, which combines a multi-channel deep neural network with SVM into a unified framework. MDSVM further learns the fusion representation and classification simultaneously to improve the generalization performance. The experimental results on the dual-view PI tasks and multi-view PI tasks of the real-world multi-view liver cancer dataset show that the proposed MPIRL achieves superior performance with an accuracy of 86.92%, sensitivity of 89.58%, and specificity of 84.25%.

Keywords: Learning using privileged information, Multi-view representation learning, Deep support vector machine, Knowledge transfer

1. Introduction

Privileged information (PI) has been successfully applied to different tasks, such as computer vision and medical image analysis Chen et al. (2022); Jiao et al. (2023); Wang et al. (2024). For example, the available imaging views of liver cancer diagnosis include B-mode ultrasound (BUS) and contrast-enhanced ultrasound (CEUS) Bharti et al. (2017). Moreover, CEUS usually consists of three views, namely Arterial Phase (AP), Portal Venous Phase (PVP), and Delayed Phase (DP) Dietrich et al. (2020). BUS is widely used for the detection and diagnosis of liver cancer by mainly providing morphological information, such as size, shape, boundary, and sonographic appearances. Due to the advancement of ultrasound contrast agents, CEUS overcomes the limitations of conventional ultrasound imaging and provides a unique approach to visualize and quantify dynamic blood perfusion. However, CEUS also suffers from time-consumption, complexity, and expensiveness in

© 2025 B. Gong & Y. Huo.

clinical practice. Therefore, the BUS is still the main view in liver cancer diagnosis, while multi-view CEUS can be taken as PI to improve the performance of BUS-based diagnostic methods.

Learning using privileged information (LUPI) is a special paradigm of transfer learning Vapnik and Izmailov (2015). LUPI aims to enhance the performance of the trained model by transferring knowledge from the PI view to the main view, in which the PI view is unavailable at the testing stage. Now, a variety of LUPI-based algorithms have been proposed and utilized for PI tasks Shu et al. (2022); Wang et al. (2024). However, the existing methods mainly focus on the classifier-level LUPI and single-view PI tasks. Therefore, the unexplored challenge in these methods is representation learning by transferring multi-view PI to improve the main view.

In recent years, deep canonical correlation analysis (DCCA) combining CCA with deep neural network (DNN) learns a complex nonlinear mapping of multi-view data by maximizing correlation. Moreover, some efforts have taken DCCA as a feature-level LUPI to successfully deal with PI-based tasks Li et al. (2019); Shaikh et al. (2020); Wang et al. (2020). However, DCCA is an unsupervised method, which cannot make full use of label information to improve representation learning based PI view. Further, Elmadany et al. (2016) proposed a discriminative DCCA (DDCCA), which learns the correlation representation and optimizes the similarity of intra-class and inter-class under the guidance of label information. Some researchers further designed a variety of supervised CCA algorithms and successfully applied them to different fields Liu et al. (2017); Guo and Wu (2019); Moon et al. (2022). Therefore, compared with unsupervised DCCA, the supervised DDCCA is a more effective LUPI paradigm. However, it is a challenging task to design a DDCCA-based LUPI to match the multi-view PI tasks.

In this work, we propose a novel feature-level LUPI algorithm based on multi-view PI, called multi-view privileged information-based representation learning (MPIRL), which consists of two modules, including a feature-level LUPI and a multi-view deep SVM (MDSVM) module. First, the feature-level LUPI module designs a multi-branch structure based on DDCCA, in which each branch is used to transfer the knowledge of one PI view to the main view. The module will generate new multi-view features of the main view to present more diversity and richer information. Meanwhile, DDCCA-based LUPI also improves the discriminability of the main view. Secondly, the MDSVM module further maps the multi-view features to the same space and learns the fusion representation to enhance the consistency between the multi-view. In addition, by the supervised characteristic, MDSVM forces the fusion representations to be located close to each other according to categories.

The main contribution of our proposal is shown as follows:

1) We propose a novel feature-level LUPI paradigm, which transfers multi-view privileged information to the main view and then generates rich and diverse multi-view representation. Meanwhile, it can enhance the intra-class similarity and reduce inter-class similarity simultaneously.

2) We develop the MDSVM algorithm, which combines a multi-channel DNN with SVM into a unified framework to enhance the performance of representation learning and classification. In particular, MDSVM uses the fusion network to improve the consistency of diverse features.

3) The experiments verify the feasibility of the proposed MPIRL algorithm. Additionally, the evaluation of a real-world liver cancer dataset confirms that the proposed method outperforms several existing algorithms.

2. Related Work

Learning using privileged information (LUPI). LUPI is an effective transfer learning paradigm in machine learning Vapnik and Izmailov (2015). The additional knowledge in this framework comes in the form of privileged information, which is latent information belonging to the training samples and is available at the training phase, but not at the testing phase. Recently, many LUPI-based algorithms have been proposed, such as multi-view SVM+ Tang et al. (2017), twin SVM with PI Che et al. (2021), V-SVR+ Shu et al. (2022), and so on Xu et al. (2019); Liu et al. (2022); Yang et al. (2025). Besides, LUPI has been widely used in many real-world applications, such as image recognition Smolyakov et al. (2018), image reconstruction Gao et al. (2019); Li et al. (2023a), and computer-aided diagnosis Shaikh et al. (2020); Wang et al. (2024). These studies show that LUPI effectively transfers the knowledge of the PI view to improve performance, but they mainly focus on a single-view PI. Therefore, a novel LUPI paradigm based on DDCCA is proposed to transfer multi-view PI to the main view.

Deep canonical correlation analysis (DCCA). CCA-based algorithms aim to maximize the correlation representation of the multi-view data generated by a paired projection matrix Yang et al. (2021). DCCA further combines CCA and DNN to learn a complex non-linear mapping of multi-view data by maximizing correlation. Now, DCCA-based methods have been used for different multi-view applications Deshmukh et al. (2022); Prabhakar et al. (2023), since DCCA effectively achieves knowledge transferring between views and enhances consistency across multiple views. In addition, DCCA is also explored as a feature-level LUPI method Li et al. (2019); Shaikh et al. (2020); Wang et al. (2020).

The supervised DCCA can make full use of label information to learn discriminative representation, which is a better paradigm for classification tasks on multi-view scenes Guo and Wu (2019). Some supervised DCCA algorithms have been proposed Elmadany et al. (2016) Liu et al. (2017); Moon et al. (2022), and successfully applied to different tasks, such as video event analysis Li et al. (2023b), object recognition and document classification Kumar and Maji (2024), and offline signature verification Zheng et al. (2025). Therefore, we introduce a novel feature-level LUPI paradigm based on supervised DCCA, which aims to generate rich and diverse representations by transferring multi-view PI to the main view.

Deep support vector machine (DSVM). A unified framework combining DNN with SVM effectively improves the model performance by jointly learning representation and classification simultaneously. Li and Zhang (2017) proposed the deep neural mapping support vector machine for representation and classification successfully by DNN explicit mapping instead of traditional kernel mapping. Later, some variants have also been successfully proposed to prove the effectiveness of the unified framework in different applications Okwuashi and Ndehedehe (2020); Xie et al. (2023); Li and Xie (2025). These works indicate that the unified framework is feasible to improve the representation learning and classification performance.

3. Method

Figure 1 shows the overall architecture of the multi-view privileged information-based representation learning algorithm MPIRL, which consists of two modules, including feature-level LUPI and multi-view DSVM. According to the LUPI paradigm, MPIRL training uses the main view and the multi-view PI features, while MPIRL testing only requires the main view. The process of MPIRL is as follows:

1) **Feature-level LUPI module** First, feature pairs will be built by the multi-view PI features and the main view, namely MV&PV1, MV&PV2, and MV&PV3. Secondly, each pair is fed into DDCCA to transfer PI to the main view, and the corresponding PI network (PIN_1/2/3) and PI features (M_P1/2/3) are extracted.

2) **Multi-view DSVM module** Due to LUPI, MDSVM requires different inputs during training and testing. MDSVM aims at learning fusion representation and classification based on the multi-view PI features. It is worth noting that the inputs of MDSVM only require the main view at the testing phase.

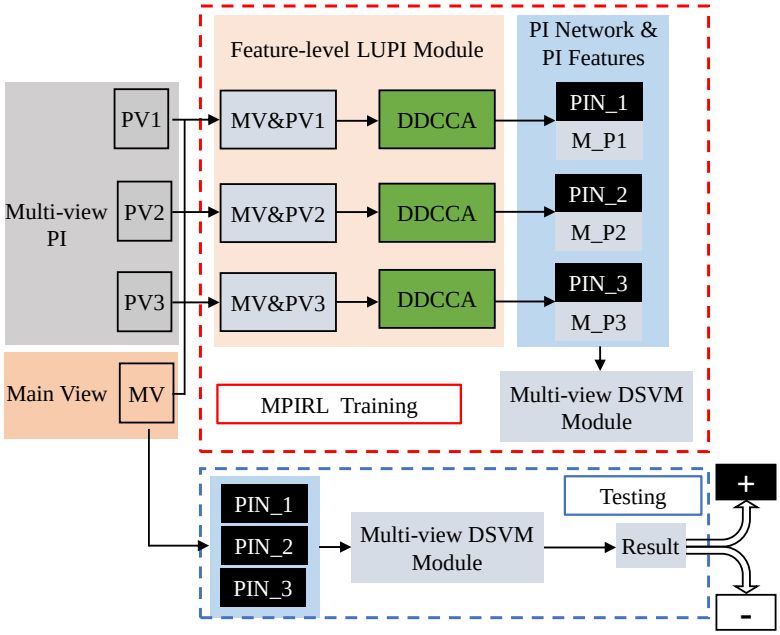

Figure 1: The overall architecture of multi-view privileged information-based representation learning. Two modules are included: Feature-level LUPI module for training PI network and generating PI features; And multi-view DSVM module for learning high-level fusion representation and classification. Note that the main view is the only requirement at the testing stage (blue dashed box).

3.1. Feature-level LUPI Module

The feature-level LUPI module uses DDCCA as a privilege method to learn the multi-view PI features. DDCCA consists of a two-channel DNN, in which one channel is for the main view and another channel is for the PI view. For each channel, DNN provides the capacity of learning high-level effective representations. Meanwhile, the correlation of the main view and PI view is guaranteed by DDCCA, which maximizes the correlation of the output. In addition, under the guidance of label information, DDCCA enlarges the intra-class similarity and decreases inter-class similarity. For simplicity, the two-channel DNN of DDCCA is denoted by X and Y, corresponding to the main view and PI view. Finally, X-channel DNN will be used for the subsequent classification module, which is called the privileged information network (PIN).

Let N samples dataset $(X, Y) \in R^{n_1 \times N} \times R^{n_2 \times N}$ denote dual-view instance with dimension n_1 and n_2 respectively. The column vectors $x_i \in R^{n_1}$ and $y_i \in R^{n_2}$ are derived from an unknown (underlying) distribution D_1 and D_2. For X and Y, their covariance matrices are $\sum_{XX}$ and $\sum_{YY}$, and cross-covariance matrix is $\sum_{XY}$. CCA finds linear projections of the double-view instance to k-pairs of vector, which are reorganized as two matrices, namely $\left(A_1^T X, A_2^T Y\right), A_1 \in R^{n_1 \times k}, A_2 \in R^{n_2 \times k}$ that are maximally correlated for each pair of the column vectors. The objective function of CCA is formulated as follows:

$$\begin{aligned} \max \quad & tr(A_1^T \sum\nolimits_{XY} A_2) \\ s.t. \quad & A_1^T \sum\nolimits_{XX} A_1 = A_2^T \sum\nolimits_{YY} A_2 = I \end{aligned} \tag{1}$$

where symbol "I"is an identity matrix with k-by-k.

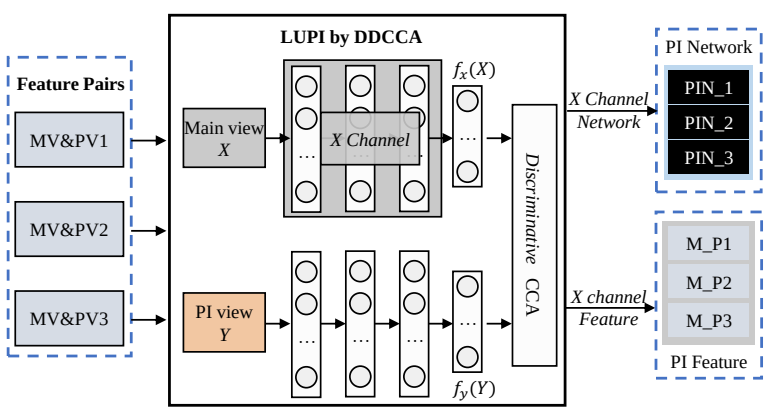

Figure 2: The feature-level LUPI flowchart by DDCCA. Three groups dual view features are fed to privileged networks module respectively to generate the PI feature (M_P1, M_P2, M_P3) and PI network (PIN_A, PIN_P, and PIN_D).

For classification problem, DDCCA reorganizes the training dataset $X = [X^1, X^2]$, $Y = [Y^1, Y^2]$, in which $X^c \in R^{d_1 \times n_c}$, $Y^c \in R^{d_2 \times n_c}$, $c \in \{1, 2\}$, $n_1 + n_2 = N$, X^c and Y^c share the same label. In DDCCA, the output layer uses Discriminative CCA to learn the

correlation representation, and enlarge intra-class similarity and intre-class similarity. For given feature X (main view), the outputs of the i-layer in the L-layer DNN is given by

$$f_i(X) \;=\; \sigma(W_i^f X + b_i^f) \tag{2}$$

where W_i^f is a matrix of weights, b_i^f is the a vector of biases, and σ is a activation function. The network for another feature Y (PI view) is built in the same way. In supervised manner, DDCCA learns the correlation representation, which is given by

$$\begin{aligned} &\max_{\{\theta_x,\theta_y\}} \omega_1^T f_x(X) M f_y(Y) \omega_2 \\ &s.t. \qquad \omega_1^T f_x(X) f_x(X)^T \omega_1 = \omega_2^T f_y(Y) f_y(Y)^T \omega_2 = 1 \end{aligned} \tag{3}$$

where θ_x and θ_y are the set of DNN parameters. $f_x(\cdot)$ and $f_y(\cdot)$ denote the X and Y channel network of DDCCA. M is a block diagonal matrix according to $X = [X^1, X^2]$, $Y = [Y^1, Y^2]$. Let $I_{n_c \times n_c}$ be a matrix with all 1 elements, and then M is written by

$$M = \begin{bmatrix} I_{n_1 \times n_1} & 0 \\ 0 & I_{n_2 \times n_2} \end{bmatrix} \tag{4}$$

After training, the LUPI module generates the PI network and PI feature based on the X channel network (as shown in Figure 2).

3.2. Multi-view DSVM

The classifier module of MPIRL is designed by combining a multi-view DNN and SVM into a unified framework, called multi-view deep SVM (MDSVM). The overall architecture of MDSVM is shown in Figure 3. MDSVM consists of three subparts: multi-channel DNN, fusion DNN, and SVM output. The subpart of the multi-channel DNN learns the high-level representation based on the PI-based feature representation from different views. Meanwhile, the PI networks of the LUPI module (PIN_1, PIN_2, and PIN_3) are used to initialize the multi-channel DNN to enhance training efficiency. The subpart of the fusion DNN is capable of further extracting the fused representation. Finally, the subpart of the SVM output is capable of conducting effective classification.

Given a dataset $T = \{(x_1, y_1), (x_2, y_2), ..., (x_N, y_N)\}$, where x_i is the main view feature, and $y_i \in \{-1, +1\}$ is the corresponding label, $i = 1, ..., N$. We further organize the input and the corresponding output by $X \in R^{d \times N}$ and $Y \in R^{1 \times N}$, respectively. By PIN_1/2/3, the generated PI feature is denoted as X^v, where $v \in \{1, 2, 3\}$ is the number of views. By transferring the privileged network (PIN_1, PIN_2, PIN_3) to MDSVM network, the procedure of learning is followed as:

The multi-channel DNN learns the different feature representations on PI feature. The encoding function in the *l-th* layer of DNN for input view X^v is given by

$$X^v \rightarrow h^{v,L} : h^{v,l} = \sigma((W^{v,l})^T h^{v,l-1} + b^{v,l}) \tag{5}$$

where $h^{v,0} = X^v$, $v = 1, ..., V$, $l = 1, ..., L$ ($V = 3$, $L = 3$ in Figure 3), σ is the activation function $1/(1 + exp(-x))$, and $h^{v,l}$, $W^{v,l}$ and $b^{v,l}$ are the hidden vector, weight matrix and

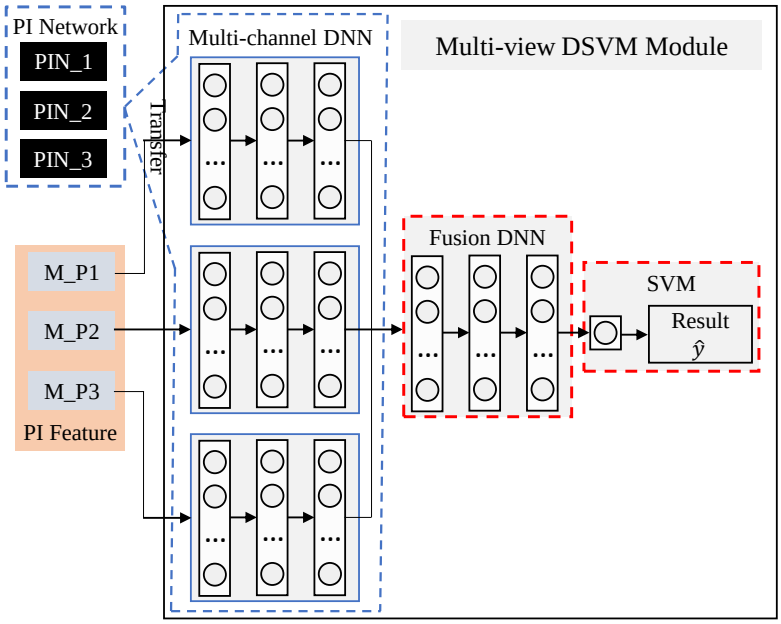

Figure 3: The architecture of our multi-view DSVM. Multi-channel DNN, fusion DNN, and SVM are integrated into a unified framework, which jointly learns the high-level fusion representation and classification.

bias, respectively. It is worth noting that the initial $W^{v,l}$ and $b^{v,l}$ come from the PIN transferred networks.

The fusion DNN fuses the multi-view feature to generate the higher-level feature representations. Firstly, the all learned features of multi-view DNNs are fed to the subpart of fusion DNN,

$$h^{1,L}, h^{2,L}, h^{3,L} \rightarrow h^1 : h^1 = \sigma(\sum_{v=1}^{V}(W^{v,L+1})^T h^{v,L} + b^{v,L+1}) \tag{6}$$

where h^1 is the first layer of fusion DNN. For others layer, it has the similar encoding function by

$$h^1 \rightarrow h^K : h^k = \sigma((W^k)^T h^{k-1} + b^k) \tag{7}$$

where h^k $(k = 2, ..., K)$ is the feature in k-th layer fusion network.

In the top layer, the final generated feature representation is fed to $L2$-SVM that has only one binary unit with the predictive value $\hat{y}$ as

$$\hat{y} = (W^{K+1})^T h^K + b^{K+1} \tag{8}$$

By introducing the $L2$-SVM, the final optimized function of MDSVM is formalized as

$$F: \quad \min_{\theta} \frac{1}{2} \left\| W^{K+1} \right\|^2 + C \sum_{y} [1 - y\hat{y}]_+^2 \tag{9}$$

where $[\cdot]_+$ is the hinge function, θ is the parameter set including the all weights and biases of MDSVM.

To improve the predictive accuracy, MDSVM is trained by a two-stage training strategy, which includes the bottom-up DNN mapping by the layer-wise pre-training in an unsupervised manner and the top-down fine-tuning in a supervised manner. The basic idea of the two-stage is inspired by deep neural network learning, which is an effective training method Hinton et al. (2006); Li and Zhang (2017). The whole procedure of the MPIRL is summarized in Algorithm 1.

Algorithm 1 Multi-view privileged information-based representation learning (MPIRL)

Input: Dataset T with one main view and multi-view privileged information;
Output: MDSVM weights, denoted as θ.
(a) **Feature-level LUPI module** Train three group DDCCA to extract three privileged networks, namely PIN_A, PIN_P, and PIN_D;
(b) **MDSVM**
(Unsupervised pre-training)
Initiate the multi-channel DNN by PIN networks;
Initiate the fusion DNN by layer-wise RBM;
(Supervised fine-tuning)
for *t from 1 to Max_iter* **do**
  for *i from 1 to N* **do**
    For given sample x_i, its gradients are calculated, denoted as $\partial L_i^{v,l}$ and ∂L_i^k according to Eq. 6 – Eq. 9;
  end
  Update parameters θ;
end
Result: Return parameters $\hat{\boldsymbol{\theta}}$.

4. Experiment Design

To validate the performance of the proposed MPIRL algorithm, a real-world multi-view liver cancer dataset with the diagnostic label is used to conduct the experiments. After the description of the dataset, we report and analyze the experimental results in detail.

Dataset. The dataset of liver cancer includes a total of 153 multi-view ultrasound data. The dataset comes from a real-world hospital. Moreover, approval from the ethics committee of the hospital was obtained, and all patients had signed informed consent. The dataset was respectively sampled from 76 and 77 patients with benign liver tumors and malignant liver tumors. The ultrasound data of each patient consists of two parts, namely BUS and CEUS. Both BUS and CEUS images were simultaneously sampled by an experienced radiologist by a LOGIQ E9 ultrasound scanner (GE Healthcare, Milwaukee, WI) with a 1-5M curved-array transducer. Sonovue (Bracco, Milan, Italy) was administrated through an acubital vein with a dose of 1.5ml. Note that CEUS includes three views, namely the Arterial Phase (AP), Portal Venous Phase (PVP), and Delayed Phase (DP).

Experiment Design. In order to demonstrate the effectiveness of our MPIRL, extensive experiments are conducted on the following aspects.

Firstly, the dual-view PI tasks are used to compare MPIRL and several classical algorithms, including: a) SVM and DSVM: the typical SVM Bottou and Lin (2007) and a method Li and Zhang (2017) by combining DNN with SVM are used for classification on the main view. b) SVM+: a classifier-level LUPI algorithm Vapnik and Izmailov (2015); c) DDCCA + SVM/DSVM: a two-stage LUPI paradigm, in which DDCCA Elmadany et al. (2016) is taken as a feature-level LUPI. Note that the experiments take BUS as the main view, while dual-view privileged information is from the concatenated feature of AP&PVP, AP&DP, and PVP&DP.

Secondly, the multi-view PI tasks are used to compare MPIRL and the state-of-the-art algorithms, including: a) SVM/DSVM (Concatenation): the main view and the multi-view privileged information are concatenated into a feature vector and then fed into classifier; b) SVM+ (Concatenation): multi-view privileged information are concatenated into single-view privileged information, and then transfer the information of the concatenate feature to the main view; c) DDCCA+SVM/DSVM: multi-view privileged information are concatenated into single-view privileged information, and then only one branch DDCCA transfer the privileged information to the main view and then SVM/DSVM are used for classification.

Thirdly, we conduct an ablation experiment to verify the effectiveness of MPIRL by comparing it with the following algorithm: 1) without supervised LUPI: the DDCCA will be replaced by an unsupervised DCCA, denoted by DCCA+MDSVM, and then the experiments of multi-view privileged information are conducted; 2) without MDSVM: the multi-view DSVM module will be removed, so the multi-view PI features will be concatenated into a single-view vector and classified by SVM and DSVM, denoted by DDCCA+SVM/DSVM (Con).

Fourthly, the hyperparameter sensitivity analysis: MPIRL algorithm involves two important parameters, namely trade-off parameter C and the hidden nodes hid_K0, in which they are selected from the sets {0.01, 0.1, 1, 10, 100, 1000} and {50, 70, 100, 150, 200, 300, 500}, respectively. In each experiment, we only change one parameter while holding the remaining parameters fixed.

Finally, in order to investigate the MPIRL for learning expressive representation, we provide a more intuitive evaluation by representation visualization in a low-dimensional embedding space. All feature representation is mapped to a 2-dimensional space by t-SNE.

Evaluation. A 5-fold cross-validation strategy is employed for performance evaluation and comparison to avoid the sampling bias introduced by a random partitioning of the dataset. The variety of indices is calculated to evaluate the comprehensive performance, including classification accuracy (ACC), sensitivity (SEN), specificity (SPE), and Youden index (YI). Moreover, the receiver operating characteristic (ROC) curve and the area under the ROC curve (AUC) are also used for evaluation. Results were given by the format of the mean $\pm$ SD (standard deviation) and the results in boldface are better than those of other algorithms.

5. Experimental Results

In this section, we demonstrate the experimental results to present the effectiveness of MPIRL in the tasks of dual-view and multi-view privileged information.

5.1. Performance Comparison of Dual-view PI Tasks

Table 1 shows the classification results of different algorithms on the dual-view PI tasks, in which the boldface means the best results. The experimental results show that, compared with other algorithms, MPIRL achieves the best results on all evaluation indices. In addition, it can be observed that 1) our MPIRL outperforms the classifier-level LUPI method SVM+, indicating that MPIRL benefits from expressive representation by the multi-branch feature-level LUPI, which improves the main view by transferring the multi-view PI;2) compared to two-stage LUPI methods (DDCCA+SVM/DSVM), our MPIRL exhibits better results with the improvement of 1% at least for evaluation indices ACC and YI, which suggests the effectiveness of representation and classification under a unified framework; 3) MPIRL is also superior to the baseline SVM/DSVM with the improvement of 4% at least for all indexes. Summarily, the competitive results of MPIRL are from two aspects: on the feature-level LUPI effectively transfers the multi-view PI to the main view to generate the diverse representation and MDSVM in a unified framework jointly learns representation and classification.

Table 1: Classification results of the dual-view PI tasks. The best classification results are highlight in boldface. (Unit: %)

Method	PI	ACC	SEN	SPE	YI
SVM	–	78.45 ± 5.32	79.33 ± 6.72	77.58 ± 6.12	56.91 ±10.78
DSVM	–	79.12 ± 6.22	79.33 ± 4.80	78.92 ± 9.94	58.25 ±12.55
SVM+	AP&PVP	81.74 ± 4.14	81.83 ± 2.77	81.67 ± 6.87	63.50 ± 8.33
DDCCA+SVM		82.94 ± 4.57	81.75 ± 5.73	84.17 ± 3.82	65.92 ± 9.13
DDCCA+DSVM		83.67 ± 3.87	83.25 ± 6.99	84.25 ± 5.77	67.50 ± 7.76
MPIRL		**84.95 ± 3.82**	**85.67 ± 5.45**	**84.25 ± 3.33**	**69.92 ± 7.55**
SVM+	AP&DP	81.07 ± 4.09	81.91 ± 4.92	80.33 ± 9.15	62.25 ± 8.31
DDCCA+SVM		82.96 ± 3.82	83.08 ± 3.69	82.83 ± 6.11	65.91 ± 7.63
DDCCA+DSVM		83.03 ± 2.51	83.17 ± 5.47	83.00 ± 7.11	66.16 ± 4.84
MPIRL		**84.32 ± 1.33**	**84.50 ± 2.96**	**84.25 ± 3.33**	**68.75 ± 2.62**
SVM+	PVP&DP	81.05 ± 2.62	80.58 ± 4.16	81.67 ± 5.00	62.23 ± 5.23
DDCCA+SVM		82.36 ± 1.58	81.83 ± 2.77	83.00 ± 5.32	64.83 ± 3.12
DDCCA+DSVM		83.65 ± 2.30	83.08 ± 3.69	84.33 ± 5.22	67.41 ± 4.47
MPIRL		**84.98 ± 1.53**	**84.50 ± 2.96**	**85.58 ± 2.42**	**70.08 ± 2.96**

Figure 4 shows the ROC curves and AUC values of the MPIRL algorithm and other algorithms on the dual-view PI tasks, in which the ROC of the MPIRL is drawn by the solid red line. It can be found that the proposed MPIRL outperforms all the comparative algorithms, and its AUC values on the different dual-view PI (AP&PVP, AP&DP, and PVP&DP) are 0.8778, 0.8749, and 0.8858, respectively.

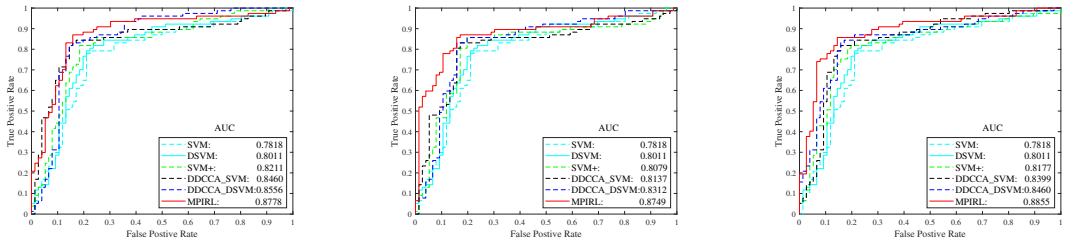

(a) PI: AP&PVP (b) PI: AP&DP (c) PI: PVP&DP

Figure 4: ROC curves and AUC values of the dual-view PI tasks.

5.2. Performance Comparison of Multi-view PI Tasks

Table 2 shows the classification results of the proposed MPIRL and the compared algorithms for multi-view PI tasks. It can be found that the MPIRL algorithm achieves the highest results with ACC $86.92 \pm 3.28\%$, SEN $89.58 \pm 3.63\%$, SPE $84.25 \pm 3.34\%$, and YI $73.83 \pm 6.47\%$. Especially, compared with SVM+, which is a classifier-level LUPI method, MPIRL achieves the improvement of 3.89%, 3.75%, 3.84%, and 7.59% on the ACC, SEN, SPE, and YI, respectively. These results show that the MPIRL algorithm effectively transfers the multi-view PI to the main view and learns the diverse representation to improve the generalization performance.

Compared with single-branch DDCCA + SVM/DSVM, which transfers the concatenated PI vector to the main view, MPIRL achieves an improvement of at least 1.98%, 2.41%, 1.25%, and 3.66% on the ACC, SEN, SPE, and YI, respectively. Therefore, the multi-branch LUPI paradigm in MPIRL learns the diverse representation and improves the sample separability. In addition, MPIRL also outperforms SVM/DSVM classification based on the concatenated features of the main view and multi-view PI, in which the accuracy improvement is more than 3.9%. In one word, the multi-branch LUPI and MDSVM in a unified framework effectively improve the performance of the MPIRL algorithm.

Table 2: Classification results of the multi-view PI tasks. The best classification results are highlight in boldface. (Unit: %)

Method	PI	ACC	SEN	SPE	YI
SVM	–	81.07 ± 4.05	83.17 ± 3.23	78.91 ± 7.38	62.08 ± 8.32
DSVM	–	82.98 ± 2.83	84.50 ± 5.56	81.58 ± 5.53	66.08 ± 5.83
SVM+	CEUS	83.03 ± 2.52	85.83 ± 4.99	80.41 ± 7.32	66.24 ± 4.88
DDCCA+SVM		83.67 ± 5.11	85.75 ± 5.35	81.58 ± 5.53	67.33 ± 4.45
DDCCA+DSVM		85.03 ± 5.27	87.17 ± 6.05	83.00 ± 7.11	70.17 ±10.47
MPIRL		**86.92 ± 3.28**	**89.58 ± 3.63**	**84.25 ± 3.34**	**73.83 ± 6.47**

Figure 5 shows the ROC curves and the corresponding values of AUC of the multi-view PI tasks, in which the ROC curve of MPIRL is drawn by the solid red line, and the corresponding AUC is exhibited on the bottom-right. It can be found that our proposed

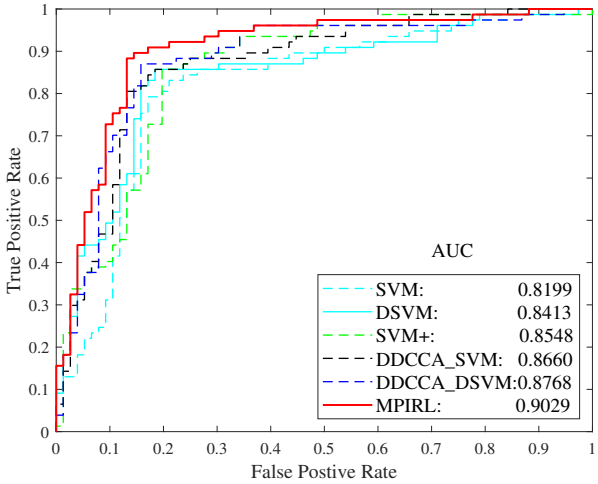

Figure 5: ROC curves and AUC values of the multi-view PI tasks.

MPIRL achieves the AUC value of 0.9029, which is superior to all the examined algorithms. This shows that MPIRL is effective for the multi-view PI tasks.

5.3. Ablation Studies

Table 3 shows the classification results of ablation studies, including unsupervised DCCA + MDSVM and supervised DDCCA + SVM/DSVM (concatenation). The experimental results illustrate the effectiveness of the proposed MPIRL from two aspects: supervised LUPI and fusion representation. Firstly, benefiting from supervised LUPI to extract richer and more diverse PI information, the classification performance of MPIRL is improved compared with the DCCA+MDSVM, which learns the multi-view PI features in the manner of the unsupervised LUPI. Secondly, compared with DDCCA+SVM/DSVM classified by the concatenated PI features, our MPIRL obtains superior performance by MDSVM to further learn the fusion representation in a unified framework. Therefore, by combining feature-level LUPI in a supervised manner and multi-view DSVM, our MPIRL can generate the more expressive representations and be trained better.

Table 3: Classification results of the ablation studies. (Unit: %)

Method	ACC	SEN	SPE	YI
DCCA+MDSVM	85.63 ± 4.31	88.16 ± 7.27	83.00 ± 7.11	71.16 ± 8.37
DDCCA+SVM(Con)	84.30 ± 3.59	85.83 ± 4.99	82.83 ± 3.89	68.66 ± 7.27
DDCCA+DSVM(Con)	85.59 ± 2.06	88.25 ± 5.63	82.92 ± 3.46	71.17 ± 4.11
MPIRL	**86.92 ± 3.28**	**89.58 ± 3.63**	**84.25 ± 3.34**	**73.83 ± 6.47**

5.4. Parameter Analysis

Figure 6 shows the classification results of MPIRL with different values of C and hidden nodes, in which it can be found that the classification results achieve the best value if C equals 10^{-1} and hidden nodes are 70. Particularly, as the hyperparameter C increases, the accuracy trends of first increasing and then decreasing (Figure 6 (a)). Meanwhile, the difference between the best result and the lowest result is small, indicating that MPIRL is low sensitive to parameter C. For parameter hidden nodes, Figure 6 (b) shows that MPIRL can be trained well if nodes are selected from 70 to 100, indicating that the optimal number of hidden nodes is easy to obtain. In one word, due to low sensitivity, the best hyperparameter can be obtained quickly to train MPIRL well.

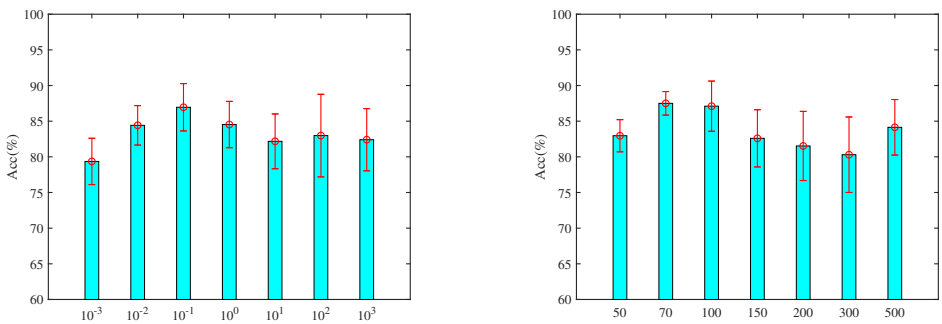

(a) C (b) hidden nodes

Figure 6: The hyperparameter sensitivity analysis.

5.5. Visualization of Feature Representation

Figure 7 shows the visualization results of representation learning, in which t-SNE maps the representation to 2D space. Figure 7 (a) is the original features mapping, which indicates that the positive and negative instances are hardly separated on a 2D projection plane.

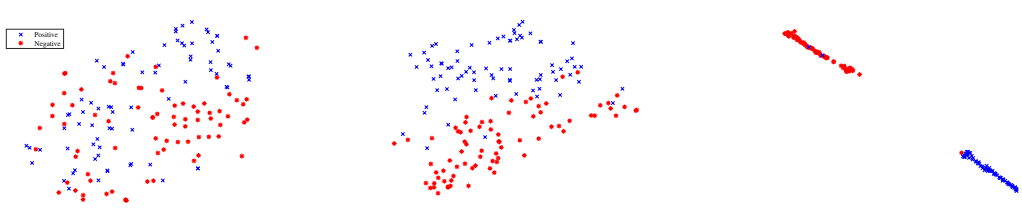

(a) Raw feature (b) Multi-channel DNN feature (c) Fusion DNN feature

Figure 7: Visualization of representation learning is obtained by t-SNE. Subfigure (a) is from the original multi-view features. Subfigure (b) and (c) present the t-SNE projection of the multi-channel DNN and fusion DNN in our MPIRL.

As shown in Figure 7 (b), in the multi-channel DNN, the mapping outputs with different categories are pushed in the opposite direction, namely blue ‘ x ’ to up and red ‘ $*$ ’ to down. Further, through the fusion DNN (Figure 7 (c)), the significant separability of representation is achieved. These results demonstrate that MPIRL effectively enhances the expressiveness of representation in the feature mapping space.

6. Conclusion

We propose a feature-level LUPI algorithm, namely MPIRL, which first uses multi-branch DDCCA to transfer privileged information to the main view and then applies MDSVM for representation learning and classification jointly. Especially, during training, DDCCA is taken as the LUPI paradigm, and multi-branch DDCCA under the guidance of the label information transfers the multi-view PI to the main view, which learns the diverse features, and increases/decreases the intra-class/inter-class similarity simultaneously. Further, MDSVM in a unified framework learns the high-level fusion representation to enhance classification performance. Moreover, during testing, the LUPI paradigm of MPIRL only requires the main view as input, while it achieves a competitive generalization performance compared with the methods used in the completed view. Experimental results show that the proposed MPIRL outperforms all the comparative algorithms on the dual-view PI tasks and multi-view PI tasks. It indicates that MPIRL has the potential for the scene of the uncompleted view in testing.

References

P. Bharti, D. Mittal, and R. Ananthasivan. Computer-aided characterization and diagnosis of diffuse liver diseases based on ultrasound imaging: a review. *Ultrasonic Imaging*, 39 (1):33–61, 2017.

L. Bottou and C.-J. Lin. Support vector machine solvers. *in Large-Scale Kernel Machines*, pages 1–27, 2007.

Z. Che, B. Liu, Y. Xiao, and H. Cai. Twin support vector machines with privileged information. *Information Sciences*, 573:141–153, 2021.

C. Chen, Q. Dou, Y. Jin, and et al. Learning with privileged multimodal knowledge for unimodal segmentation. *IEEE Transactions on Medical Imaging*, 41(3):621–632, 2022.

S. Deshmukh, A. Abhyankar, and S. Kelkar. DCCA and DMCCA framework for multimodal biometric system. *Multimedia Tools and Applications*, 81(17):24477–24491, 2022.

C. F. Dietrich, C. P. Nolsoe, R. G. Berzigotti, and et al. Guidelines and good clinical practice recommendations for contrast enhanced ultrasound (ceus) in the liver–update 2020–wfumb in cooperation with efsumb, afsumb, aium, and flaus. *Ultraschall in der Medizin-European Journal of Ultrasound*, 41(05):562–585, 2020.

N. E. D. Elmadany, Y. He, and L. Guan. Multiview learning via deep discriminative canonical correlation analysis. In *IEEE International Conference on Acoustics, Speech and Signal Processing (ICASSP)*, pages 2409–2413, 2016.

Z. F. Gao, S. T. Wu, Z. Liu, and et al. Learning the implicit strain reconstruction in ultrasound elastography using privileged information. *Medical Image Analysis*, 58:101534, 2019.

C. Guo and D. R. Wu. Canonical correlation analysis (CCA) based multi-view learning: An overview. *arXiv preprint arXiv:1907.01693*, 2019.

G. Hinton, S. Osindero, and Y. Teh. A fast learning algorithm for deep belief nets. *Neural Computation*, 18(7):1527–1554, 2006.

W. Jiao, S. Song, H. Han, and et al. Artificially intelligent differential diagnosis of enlarged lymph nodes with random vector functional link network plus. *Medical Engineering and Physics*, 111:103939, 2023.

D. Kumar and P. Maji. Discriminative deep canonical correlation analysis for multi-view data. *IEEE Transactions on Neural Networks and Learning Systems*, 35(10):14288–14300, 2024.

Q. Li, Z. Y. Shen, Q. Li, and et al. Privileged anatomical and protocol discrimination in trackerless 3D ultrasound reconstruction. *In International Workshop on Advances in Simplifying Medical Ultrasound*, pages 142–151, 2023a.

X. Li, L. Zhang, and Zhang. Multi-view discriminative fusion on canonical correlation analysis in event classification. *International Conference on Computer Research and Development (ICCRD)*, pages 151–155, 2023b.

Y. Li, F. Q. Meng, J. Shi, and et al. Learning using privileged information improves neuroimaging-based cad of Alzheimer's disease: a comparative study. *Medical and Biological Engineering and Computing*, 57:1605–1616, 2019.

Y. F. Li and X. J. Xie. Two novel deep multi-view support vector machines for multiclass classification. *Applied Intelligence*, 55(2):1–17, 2025.

Y. J. Li and T. Zhang. Deep neural mapping support vector machines. *Neural Networks*, 93:185–194, 2017.

B. Liu, L. Liu, Y. Xiao, and et al. AdaBoost-based transfer learning with privileged information. *Information Sciences*, 593:216–232, 2022.

Y. Liu, Y. Li, Y. H. Yuan, and et al. Supervised deep canonical correlation analysis for multiview feature learning. *International Conference on Neural Information Processing (ICONIP)*, pages 575–582, 2017.

S. Moon, J. Hwang, and H. Lee. SDGCCA: supervised deep generalized canonical correlation analysis for multi-omics integration. *Journal of Computational Biology*, 29(8):892–907, 2022.

O. Okwuashi and C. E. Ndehedehe. Deep support vector machine for hyperspectral image classification. *Pattern Recognition*, 103:107298, 2020.

G. A. Prabhakar, B. Basel, A. Dutta, and C. V. R. Rao. Multichannel CNN-BLSTM architecture for speech emotion recognition system by fusion of magnitude and phase spectral features using DCCA for consumer applications. *IEEE Transactions on Consumer Electronics*, 69(2):226–235, 2023.

T. A. Shaikh, R. Ali, and M. S. Beg. Transfer learning privileged information fuels CAD diagnosis of breast cancer. *Machine Vision and Applications*, 31:9, 2020.

Y. Shu, Q. Li, C. Xu, and et al. V-SVR+: Support vector regression with variational privileged information. *IEEE Transactions on Multimedia*, 24:876–889, 2022.

D. Smolyakov, N. Sviridenko, E. Bruikov, and E. Burnaev. Anomaly pattern recognition with privileged information for sensor fault detection. *Artificial Neural Networks in Pattern Recognition*, pages 320–332, 2018.

J. J. Tang, Y. Tian, P. Zhang, and X. Liu. Multiview privileged support vector machines. *IEEE Transactions on Neural Networks and Learning Systems*, 29(8):3463–3477, 2017.

V. Vapnik and R. Izmailov. Learning using privileged information: similarity control and knowledge transfer. *Journal of Machine Learning Research*, 16:2023–2049, 2015.

Q. Wang, H. Lian, G. Sun, and et al. iCmSC: Incomplete cross-modal subspace clustering. *IEEE Transactions on Image Processing*, 30:305–317, 2020.

X. Wang, X. Ren, G. Jin, and et al. B-mode ultrasound-based CAD by learning using privileged information with dual-level missing modality completion. *Computers in Biology and Medicine*, 182:109106, 2024.

X. J. Xie, Y. F. Li, and S. L. Sun. Deep multi-view multiclass twin support vector machines. *Information Fusion*, 91:80–92, 2023.

W. Xu, W. Liu, H. Chi, and et al. Self-paced learning with privileged information. *Neurocomputing*, 362:147–155, 2019.

H. Y. Yang, M. Steinbach, G. Melton, and et al. Combining self-supervision and privileged information for representation learning from tabular data. *Knowledge and Information Systems*, pages 1–29, 2025.

X. Yang, W. Liu, W. Liu, and D. Tao. A survey on canonical correlation analysis. *IEEE Transactions on Knowledge and Data Engineering*, 33(6):2349–2368, 2021.

L. Zheng, X. Zhao, S. Xu, and et al. Learning discriminative representations by a canonical correlation analysis-based siamese network for offline signature verification. *Engineering Applications of Artificial Intelligence*, 139:109640, 2025.